POLITECNICO DI TORINO
Repository ISTITUZIONALE

Recurrent Neural Network Model for On-Board Estimation of the Side-Slip Angle in a Four-Wheel Drive and Steering Vehicle

Original
Recurrent Neural Network Model for On-Board Estimation of the Side-Slip Angle in a Four-Wheel Drive and Steering Vehicle / Giuliacci, Tiziano Alberto; Ballesio, Stefano; Fainello, Marco; Mair, Ulrich; King, Julian. - In: SAE INTERNATIONAL JOURNAL OF PASSENGER VEHICLE SYSTEMS. - ISSN 2770-3460. - 17:1(2023). [10.4271/15-17-01-0003]

Availability:
This version is available at: 11583/2982790 since: 2023-10-05T16:53:34Z

Publisher:
SAE INTERNATIONAL

Published
DOI:10.4271/15-17-01-0003

Terms of use:

This article is made available under terms and conditions as specified in the corresponding bibliographic description in the repository

Publisher copyright

(Article begins on next page)

16 May 2024

Downloaded from SAE International by Tiziano [illegible], [illegible], October 02, 2023

ARTICLE INFO
Article ID: 15-17-01-0003
© 2024 Addfor S.p.A.
doi:10.4271/15-17-01-0003

Recurrent Neural Network Model for On-Board Estimation of the Side-Slip Angle in a Four-Wheel Drive and Steering Vehicle

Tiziano Alberto Giuliacci,[1] Stefano Ballesio,[1] Marco Fainello,[1] Ulrich Mair,[2] and Julian King[2]

[1]Addfor S.p.a., Italy
[2]ZF Friedrichshafen AG, Germany

Abstract

A valuable quantity for analyzing the lateral dynamics of road vehicles is the side-slip angle, that is, the angle between the vehicle's longitudinal axis and its speed direction. A reliable real-time side-slip angle value enables several features, such as stability controls, identification of understeer and oversteer conditions, estimation of lateral forces during cornering, or tire grip and wear estimation. Since the direct measurement of this variable can only be done with complex and expensive devices, it is worth trying to estimate it through virtual sensors based on mathematical models. This article illustrates a methodology for real-time on-board estimation of the side-slip angle through a machine learning model (SSE—side-slip estimator). It exploits a recurrent neural network trained and tested via on-road experimental data acquisition. In particular, the machine learning model only uses input signals from a standard road car sensor configuration. The model adaptability to different road conditions and tire wear levels has been verified through a sensitivity analysis and model testing on real-world data proves the robustness and accuracy of the proposed solution achieving a root mean square error (RMSE) of 0.18 deg and a maximum absolute error of 1.52 deg on the test dataset. The proposed model can be considered as a reliable and cheap potential solution for the real-time on-board side-slip angle estimation in serial cars.

History

Received: 20 Feb 2023
Revised: 09 Jun 2023
Accepted: 08 Sep 2023
e-Available: 23 Sep 2023

Keywords

Machine learning, Artificial intelligence, Side-slip angle, Vehicle dynamics, Recurrent neural network, Virtual sensors, Vehicle state estimation

Citation

Giuliacci, T., Ballesio, S., Fainello, M., Mair, U. et al., "Recurrent Neural Network Model for On-Board Estimation of the Side-Slip Angle in a Four-Wheel Drive and Steering Vehicle," *SAE Int. J. Passeng. Veh. Syst.* 17(1):2024, doi:10.4271/15-17-01-0003.

ISSN: 2770-3460
e-ISSN: 2770-3479

© 2024 Addfor S.p.A. Published by SAE International. This Open Access article is published under the terms of the Creative Commons Attribution License (http://creativecommons.org/licenses/by/4.0/), which permits distribution, and reproduction in any medium, provided that the original author(s) and the source are credited.

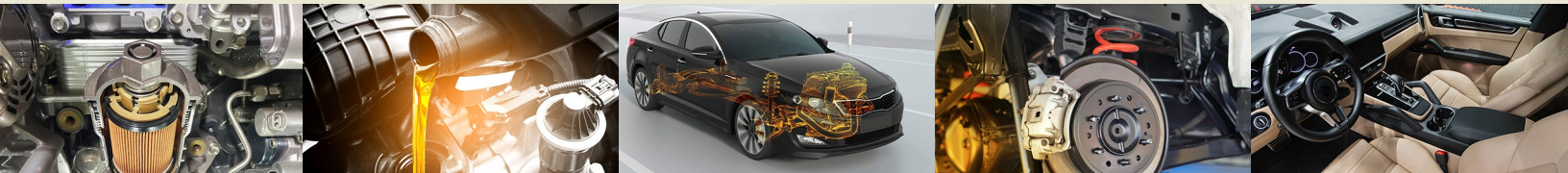

Downloaded from SAE International by Tiziano Giuliacci, Monday, October 02, 2023

Introduction

The knowledge of the side-slip angle ("beta") is crucial for improving vehicle stability and drivability and is a key point for some electronic stability controls design [1, 2, 3]. Monitoring the side-slip angle allows to predict when the vehicle is going to saturate the rear tires and lose directional stability. Furthermore, some articles prove that the side-slip angle allows for an easy identification of understeer and oversteer conditions [4]. Moreover, side-slip angle estimation can be coupled with side-slip control, for example, in performance and sport driving, which aims at keeping vehicle side slip within a certain range through different algorithms and techniques [5, 6]. In addition, due to the strong link between side-slip angle and tire operating conditions, the side-slip angle can serve as an important input for estimating the maximum friction coefficient between the tire contact patch and the road surface [7, 8, 9] or for determining tire wear [10, 11].

Obtaining a high-accuracy and robust measurement of the side-slip angle with the standard production car configuration is still a difficult task. To get an accurate measurement of this variable, expensive, complex, and well-calibrated equipment is needed, such as optical sensors or inertial platforms, coupled with differential global positioning systems using sensor fusion techniques. In this context, virtual sensing techniques have been proven as a valuable alternative solution for side-slip angle real-time estimation [12]. This methodology exploits data from a set of readily available physical sensors to determine another quantity of interest through a particular algorithm, which in this case is a model able to calculate the side-slip angle value. In general, virtual sensors may be useful in cases in which the target value is not directly measurable (for instance, the sensor cannot be placed in the proper position) or to avoid the high costs of some devices, leading to an economic advantage. In other situations, validated virtual sensors can be employed to provide redundancy required for safety reasons or to allow for early diagnostics and predictive maintenance.

In the scientific community, several algorithmic approaches have been presented to estimate the side-slip angle [13]. However, due to the strong nonlinearity of the problem and the high sensitivity of most methods to parameter variability and sensor noise, determining the side-slip angle is still considered to be a nontrivial task. The most common methodology is the extended Kalman filter (EKF) [14, 15]. In the literature different forms and applications of the Kalman filter can be found, for example, in combination with fuzzy logic [16], with the Pacejka's magic formula [17], or in other hybrid forms [18]. These model-based methodologies, known as dynamics-based approaches, require a wide range of vehicle parameters to be known or identified beforehand, thereby reducing their general applicability. An alternative method is the kinematics-based approach [19, 20], which is slightly simpler by not explicitly modeling forces between the vehicle and its environment, for example, tire forces. Its main drawback is the generally reduced precision of the side-slip angle estimation due to the required numerical integration of biased and noisy IMU signals. Mixed methodologies have been considered too, trying to achieve higher performance by merging the individual advantages of these two approaches [21, 22, 23]. In addition, different state observers [24, 25], more complex adaptive systems [8, 9, 26], and neural network (NN) approaches have been employed. Regarding the latter, the literature is mainly focused on fully connected (FNN) architectures [27], which are frequently used for regression problems. However, recurrent neural networks (RNNs) are generally preferred when dealing with dynamic systems state estimation due to several memory terms, which allow to store information about past samples [28]. Many RNN applications in the literature are used in conjunction with other methodologies such as Kalman filters [29] or sensor data fusion [30]. For further details, see Chindamo et al. for an exhaustive literary review in this context [31]. Another main drawback of NN approaches published so far is their high computational demand for on-board estimation in real time [32].

Filling in this gap, this work describes the use of a standalone RNNs model for the side-slip angle estimation, which can achieve high precision within a wide operating range including several different working conditions and which has a computational burden compatible with most of the standard automotive production ECUs. The target vehicle in the current application has a four-wheel drive and a front and rear steering system. The proposed model was tested through on-road data, considering different road grip conditions, different tire wear levels, and various driving styles. The resulting virtual sensor is perfectly able to run on most of the ECUs available in production cars, and it uses only signals provided by standard configuration sensors: longitudinal and lateral acceleration, front and rear wheel steering angles, yaw rate, and wheel speeds. Therefore, no special or additional hardware is required. Furthermore, the final trained system can compensate for a few milliseconds of latency introduced by the sensor signal acquisition system and is ready for being put into production in road homologated cars. Although the trained model is capable of handling several operating conditions, all of these must be generally included in the training dataset. Furthermore, the final model is closely related to the considered vehicle and its kinematic and dynamic properties, and a new training is required for applications in vehicles with different characteristics.

This work initially introduces the problem definition and the dataset available from on-road experiments. This dataset is composed of several maneuvers, for example, sine sweeps at different frequencies and speeds, double lane changes, steer steps involving different amplitudes, and handling laps recorded on different grip conditions and with different tire wear levels. Subsequently, the model architecture underlying the virtual sensor will be described. The final part shows and discusses the training and testing results. It is demonstrated that the proposed model can estimate the side-slip angle with a root mean square error (RMSE) of about 0.18 deg on the testing dataset.

Downloaded from SAE International by Tiziano Giuliacci, Monday, October 02, 2023

Materials and Methods

The vector V, which is the vehicle speed, can be decomposed into longitudinal and lateral velocity according to Equation 1 (Figure 1).

$$\underline{V} = v_x \underline{i} + v_y \underline{j} \quad \text{Eq. (1)}$$

When the vehicle drives straight ahead, v_y is zero and the absolute speed V is equal to v_x.

The side-slip angle β is defined as the angle between the vehicle speed vector V and the longitudinal speed vector v_x. Practically, the side-slip angle provides information about the handling characteristic of the vehicle and about the saturation of the tires and loss of control of the vehicle. It can be mathematically expressed as follows:

$$\beta = \tan^{-1}\left(\frac{v_y}{v_x}\right) \quad \text{Eq. (2)}$$

For a given curve radius, the sign of the side-slip angle β strongly depends on the longitudinal velocity v_x. While the vehicle is turning with low longitudinal velocity, the lateral acceleration is not very high, and the speed vector V points in the direction of the curve. In this situation β has a sign determined by simple vehicle kinematics. Once the vehicle speed increases, the lateral acceleration does too, and the speed vector V starts drifting outward, gradually reducing the slip angle magnitude, and finally leading to a sign change of β. This transition behavior is strongly influenced by many factors, such as the vehicle configuration (e.g., weight and balance) and the friction coefficient value between tires and road.

FIGURE 1 Vehicle body schematization.

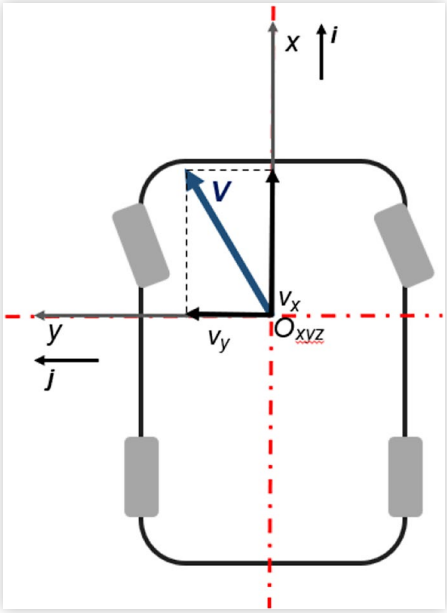

© Addfor S.p.A.

Dataset

An experimental dataset used to train the NN has been collected by performing different maneuvers in a proving ground and a handling track. The target vehicle under study was a Cadillac CT6 with all-wheel drive as well as front and rear steering. Since the standard vehicle sensor configuration cannot provide ground-truth data for the side-slip angle value, the vehicle has been equipped with an OxTS RT3000 GNS/INSS platform (Oxford Technical Solutions Inc.) [33], providing reference signals for longitudinal and lateral velocity in the center of gravity. The set of input signals (features) for the NN encompasses longitudinal and lateral acceleration (Ax/Ay) as well as the yaw rate from the vehicle's series IMU, the four wheel speeds and the front and rear wheel steering angles. All signals were recorded at a sampling frequency of 100 Hz. A set of predefined maneuvers were repeated on different grip conditions and with different wear levels for one specific tire. Hence, the dataset can be classified into four distinct classes depending on the working conditions, see Table 1.

For each working condition, both synthetic maneuvers and handling laps were performed, see Table 2. Handling laps were performed with a moderate driving style and a sportive driving style.

In Figure 2, a synthetic representation of the entire dataset available for the model training and testing is provided and in Figure 3 a frequency analysis is shown to check the signal bandwidth in frequency domain. The total length of the on-road data acquired is about 1 hour.

In Figures 4 and 5, violin plots of the side-slip angle β distribution within the different groups are presented.

The red line and the black line represent the median and the mean value of the distribution, respectively, while the figure's width represents the probability density of the data.

TABLE 1 Dataset classification depending on tire grip and wear conditions.

/	Grip level	Wear level	Time (sec)
a.	Dry road	New tires	1366
b.	Dry road	Worn tires	810
c.	Wet road	New tires	765
d.	Wet road	Worn tires	547

© Addfor S.p.A.

TABLE 2 Maneuvers performed by the driver during on-road test for each condition of tire grip and wear. For each maneuver several repetitions were acquired.

/	Maneuver	Time (sec)
A.	Steer sinus sweep	73
B.	Circle	308
C.	Steer ramp	142
D.	Double lane change (DLC)	203
E.	Handling	2762

© Addfor S.p.A.

Downloaded from SAE International by Tiziano Giuliacci, Monday, October 02, 2023

FIGURE 2 Representation of the entire on-road dataset available, showing the input signals (features) of the neural network vs. the target value β.

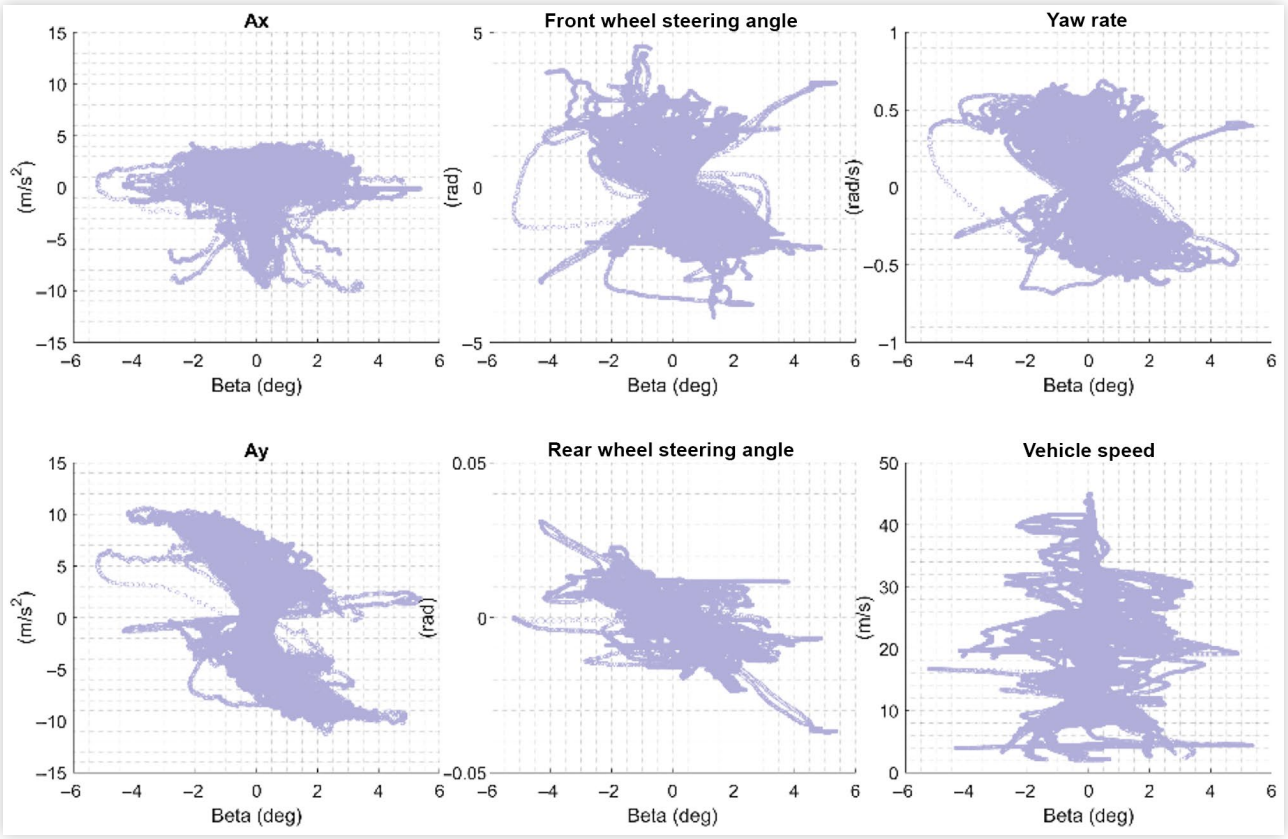

© Addfor S.p.A.

FIGURE 3 Normalized FFTs of the acquired signals of interest.

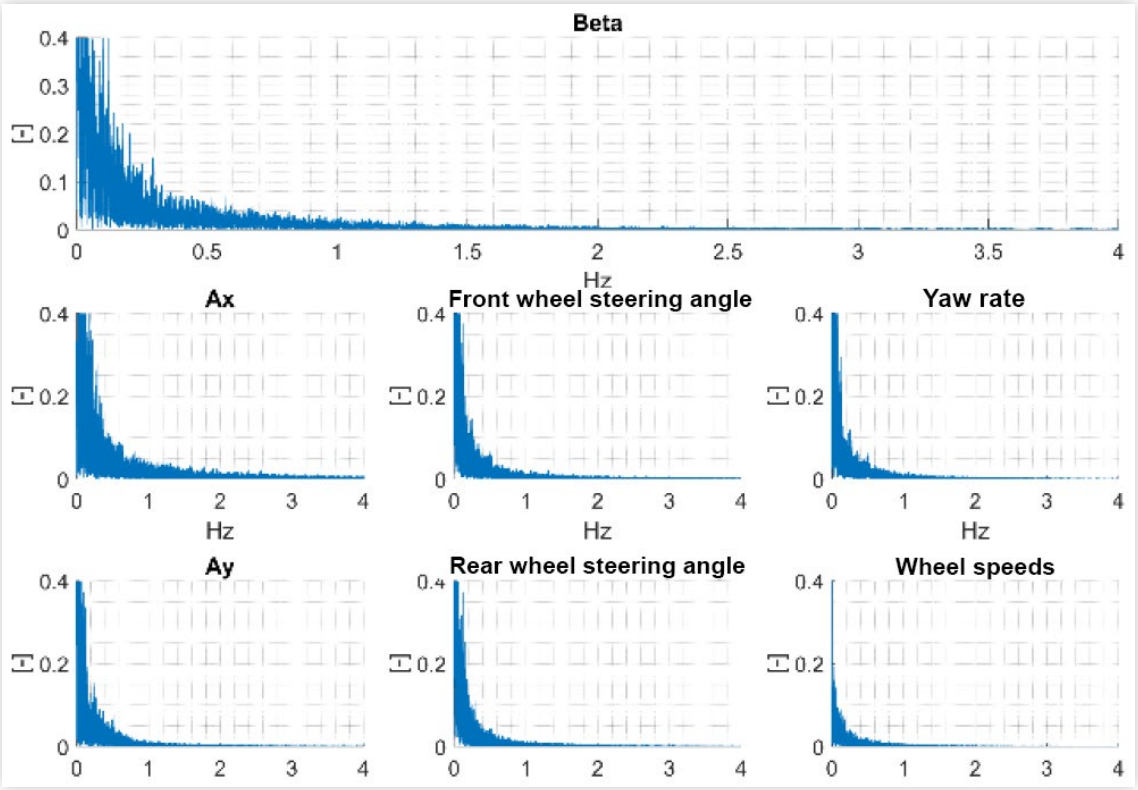

© Addfor S.p.A.

Downloaded from SAE International by Tiziano Giuliacci, Monday, October 02, 2023

FIGURE 4 Side-slip angle β distribution along the tire grip and wear classification.

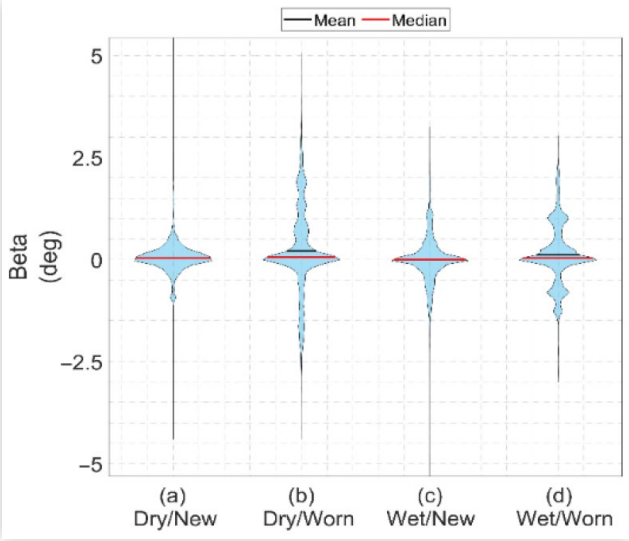

© Addfor S.p.A.

As it is shown in Figure 4, class a. and c. have mostly smaller β values, except for some outliers. A wider distribution of β is seen in classes b. and d. Considering the maneuver groups, for circle driving (B), ramp steer (C), and handling (E) maneuvers higher side-slip angles could be achieved, while β values in groups (A) and (D) are smaller in magnitude.

Before the NN model training, the dataset has undergone a phase of pre-processing: data has been controlled to analyze the sampling, and to detect anomalies such as missing values, sensor failure, or inconsistencies between the signals and the physical laws of the vehicle dynamics under the assumptions of a four-wheeled vehicle as a rigid body on a horizontal plane

FIGURE 5 Side-slip angle β distribution along driving maneuvers classification.

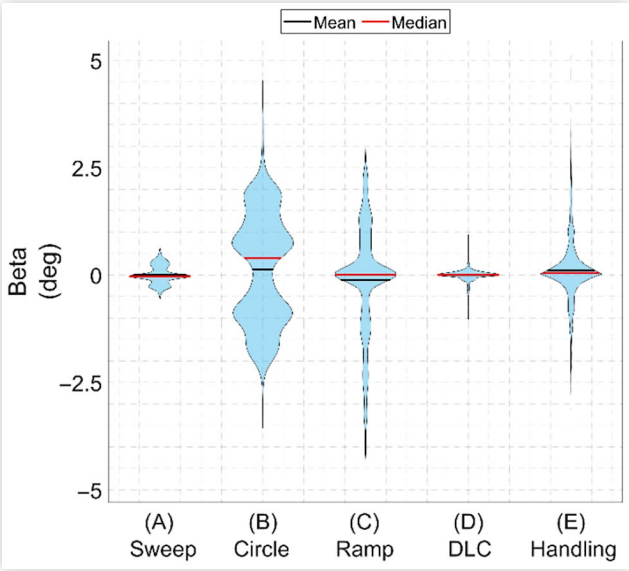

© Addfor S.p.A.

(which can be extended to an inclined plane if necessary). Data has been cleaned consequently through a proprietary software. The dataset is split into a training set, used to identify the NN parameters, and a testing set, which is kept completely separated from the training process and used only to verify the model performance. In order to create the training set, several random combinations have been done with the previously described maneuvers and the combination with a better training performance has been chosen. A train/test split ratio of about 0.30 was used, so the total on-road test length used for the model training is about 15 minutes. In this work, several parts for each condition of tire grip and wear and for each maneuver were included in the training dataset part. However, it is not mandatory to include a specific maneuver for each operating condition. Furthermore, this might not be possible due to the dataset stratification. Generally, the more comprehensive the dataset, the greater the network's ability to generalize its predictions.

Virtual Sensor Model

The proposed machine learning model for the side-slip estimation consists in a regression RNN. These types of models are meant for approximating an output signal from a set of input channels by considering linear dependencies, nonlinear dependencies, a stochastic contribution that compensates the system disturbance due to noise, and a memory term for dynamic behavior.

The model proposed works in a discrete time domain and it returns as output the side-slip angle β in degrees at time t by receiving as input the value at time t from the following standard CAN signals:

- Longitudinal chassis acceleration;
- Lateral chassis acceleration;
- Yaw rate;
- Front wheel steering angle;
- Rear wheel steering angle;
- Four wheel speeds.

These signals constitute the input vector $\underline{x}_t$ for the RNN. The network architecture consists of one hidden recurrent layer with 16 long short-term memory (LSTM) cells as presented by Gers et al. in 1999 [34] and a single output layer consisting of 10 neurons with sigmoid activation functions. LSTM cells can store information in a long-term memory state $\underline{s}_t$ by using an input gate (i), a forget gate (f), an update gate (g), and an output gate (o). The learnable parameters of the hidden layer are stored in matrices, representing the input weights (W_i, W_f, W_g, W_o), the recurrent weights (R_i, R_f, R_g, R_o), and the biases (B_i, B_f, B_g, B_o), respectively, for each gate. The gate equations are:

$$\underline{i}_t = \sigma\left(\underline{W}_i \cdot \underline{x}_t + \underline{R}_i \cdot \underline{y}_{t-1} + \underline{B}_i\right)$$

Downloaded from SAE International by Tiziano Giuliacci, Monday, October 02, 2023

$$\underline{f}_t = \sigma\left(\underline{W}_f \cdot \underline{x}_t + \underline{R}_f \cdot \underline{y}_{t-1} + \underline{B}_f\right)$$

$$\underline{g}_t = \sigma\left(\underline{W}_g \cdot \underline{x}_t + \underline{R}_g \cdot \underline{y}_{t-1} + \underline{B}_g\right)$$

$$\underline{o}_t = \sigma\left(\underline{W}_o \cdot \underline{x}_t + \underline{R}_o \cdot \underline{y}_{t-1} + \underline{B}_o\right) \quad \text{Eq. (3)}$$

where σ is a sigmoid activation function, $\underline{x}_t$ is the input at time step t, and $\underline{y}_{t-1}$ is the recurrent input calculated according to

$$\underline{y}_t = \underline{o}_t \cdot \sigma\left(\underline{s}_t\right) \quad \text{Eq. (4)}$$

At each time step, the state is updated via:

$$\underline{s}_t = \underline{f}_t \cdot \underline{s}_{t-1} + \underline{i}_t \cdot \underline{g}_t \quad \text{Eq. (5)}$$

The RNN parameters (W, R, B) are learnt from the data during the training process, which consists in minimizing the error between the predicted side-slip angle and the measured (ground-truth) side-slip angle. Hyper-parameters are defined and tuned by a trial-and-error process. The model has been trained for 100 epochs, with a batch size of 1024, through the stochastic gradient descent with momentum (s.g.d.m.) algorithm, with a starting learning rate equal to 0.0060, and a momentum coefficient of 0.893.

The results achieved, as shown subsequently, prove that this method can ensure a highly performant side-slip angle estimation within a wide and heterogeneous operating range.

Results and Discussion

The performance of the NN model for the side-slip angle estimation has been calculated by comparing the experimentally measured β with the estimated output value $\hat{\beta}$ from the model. The main metrics used to evaluate the goodness-of-fit are the RMSE and the coefficient of determination R^2, which are defined in Equations 7 and 8, respectively. Additionally, the maximum absolute error of the model has been considered, see Equation 9.

Assuming the model error ε_k for the kth sample is defined as:

$$\varepsilon_k = \beta_k - \hat{\beta}_k \quad \text{Eq. (6)}$$

the RMSE value is given by:

$$\text{RMSE} = \sqrt{\frac{\sum_{k=1}^{n} \varepsilon_k^2}{n}} \quad \text{Eq. (7)}$$

while the adjusted coefficient of determination R^2 is defined as follows:

$$\tilde{R}^2 = 1 - \frac{\sum_{k=1}^{n} \left(\varepsilon_k\right)^2}{\sum_{k=1}^{n} \left(\beta_k - \bar{\beta}\right)^2}$$

TABLE 3 Model performance expressed through RMSE, R^2, and maximum absolute error. The metrics were evaluated on both the overall dataset and training and testing datasets separately.

	RMSE (deg)	R^2 (-)	Max Abs Error (deg)
Overall	0.16	0.95	1.52
Training	0.12	0.98	1.03
Testing	0.18	0.93	1.52

© Addfor S.p.A.

$$R^2 = 1 - \frac{\left(1 - \tilde{R}^2\right)\left(n-1\right)}{\left(n-p\right)} \quad \text{Eq. (8)}$$

where n corresponds to the total number of samples considered, p corresponds to the independent variables of the model, and $\bar{\beta}$ is the mean of the measured β_k for $k = 1 \ldots n$. A value of $R^2 = 1$ corresponds to a perfect fit between the measured and predicted side-slip angle.

Finally, the maximum absolute error is:

$$\max \text{Abs Error} = \max\left(\left|\varepsilon_k\right|\right) \quad \text{Eq. (9)}$$

The model performance evaluated according to these metrics, both on the overall dataset and on the training and testing datasets separately, are shown in the Table 3. The overall dataset includes all types of operating conditions specified in Section 'Dataset'. The train/test split ratio used is about 0.3, so the total length of training dataset is only about 15 minutes.

As it can be seen, the coefficient of determination R^2 on the overall dataset is about 0.95. Separately evaluating R^2 on the training and testing data set yields a value of 0.98 and 0.93, respectively. This points toward a slight overfitting of the model to the training data, which could be alleviated by increasing the train/test split ratio. Nevertheless, as shown in Figure 6 the model regression performance on the testing data set is still good.

Figure 7 presents the error depending on the true beta value. Since the error trend is roughly constant along the whole beta domain (as reflected by a low correlation coefficient equal to 0.11), it can be concluded that the model has picked up the essential beta dynamics.

The maximum absolute error in the training and testing dataset is 1.03 deg and 1.52 deg, respectively. However, observing the error frequency distribution in Figure 8, errors with this magnitude are quite rare as the 5th- and 95th-percentile of the error in the testing dataset is about −0.27 deg and 0.32 deg, respectively.

In Figures 9 and 10 two exemplary snippets from the model testing dataset are presented. Figure 9 shows a few seconds of sportive driving on a dry asphalt handling track using worn tires, whereas Figure 10 corresponds to sportive driving on a wet asphalt handling track using a new set of tires. As it can be seen, these examples represent two

Downloaded from SAE International by Tiziano Giuliacci, Monday, October 02, 2023

FIGURE 6 Model regression performance.

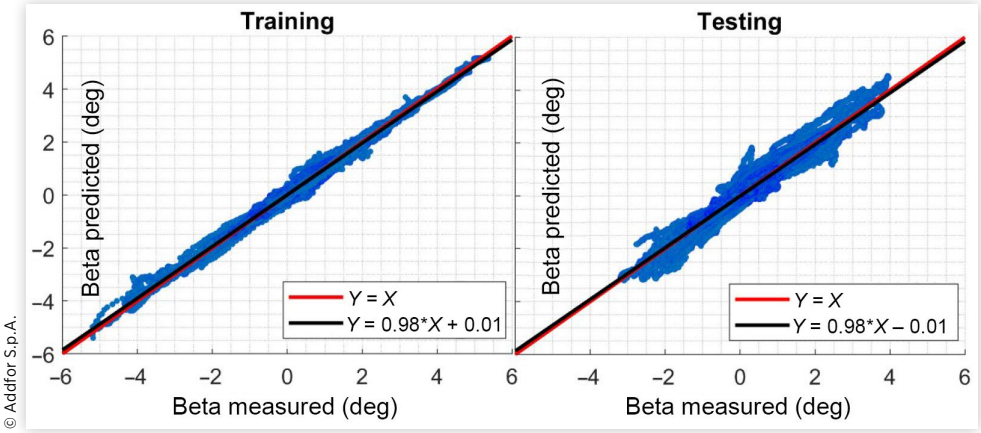

FIGURE 7 Error depending on β value. The error boxes represent the mean error value in bin regroupings of β, where the uncertainty is 1.96 times the error standard deviation (95% confidence interval). Individual error values are represented as point clouds.

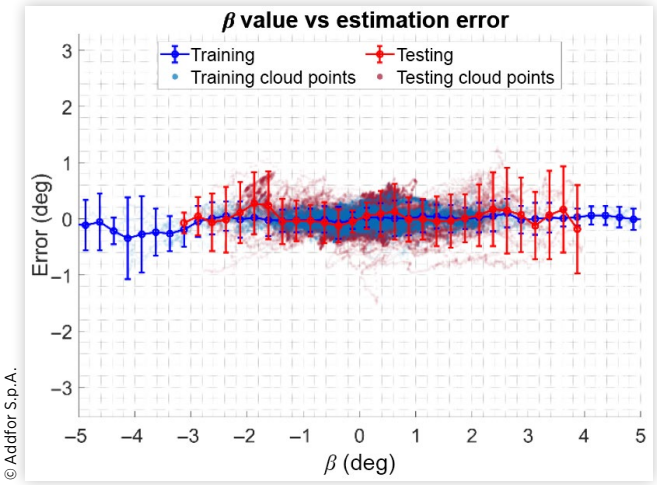

FIGURE 8 Distribution of the model error in the training and testing datasets.

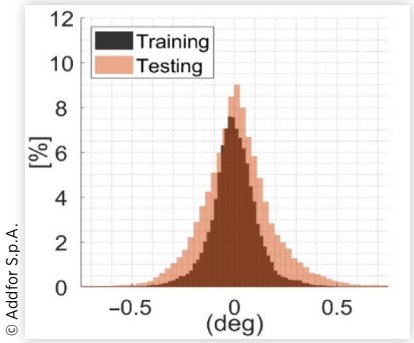

FIGURE 9 Handling sport session, in dry grip conditions and using worn tires. The upper plot shows the estimated β, in comparison with the reference data as well as the absolute error. In the following plots the input signals are represented.

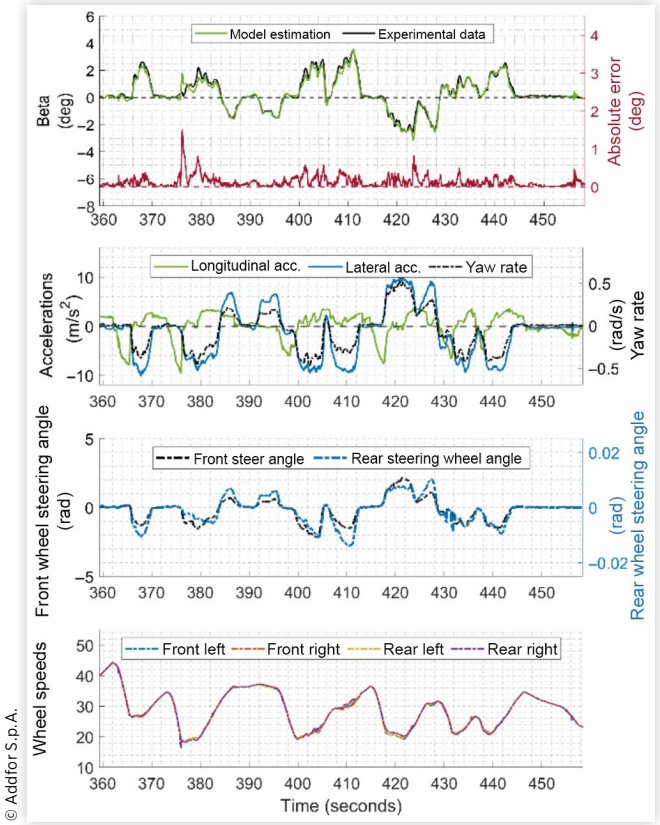

Downloaded from SAE International by Tiziano Giuliacci, Monday, October 02, 2023

FIGURE 10 Handling sport session, in wet grip conditions and using new tires. The upper plot shows the estimated β, in comparison with the reference data as well as the absolute error. In the following plots the input signals are represented.

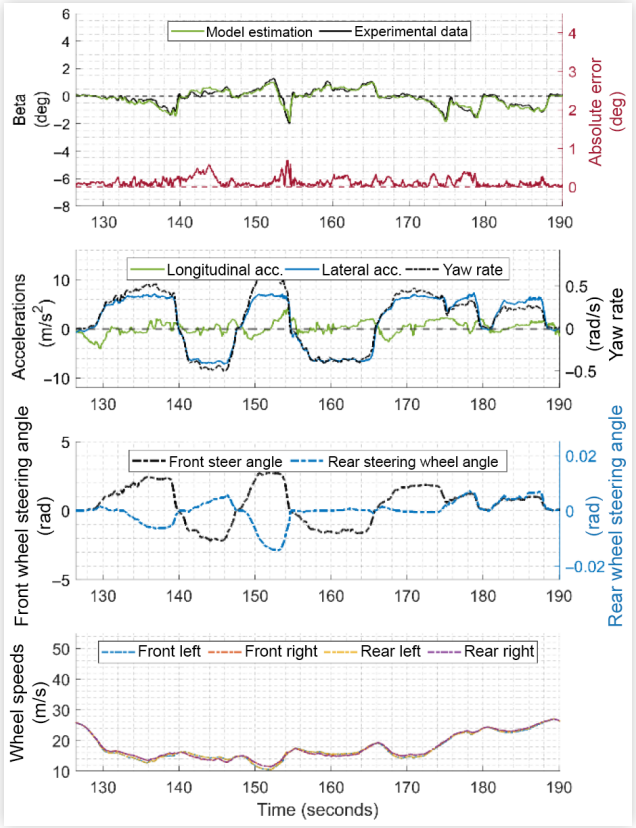

© Addfor S.p.A.

extremely different situations, and they cover almost the entire speed and side-slip angle range of the overall dataset, see also Figure 2.

The model achieves a high prediction accuracy in both the scenarios. The absolute error is almost always lower than 0.5 deg, except for a few isolated points. In Figure 11, a corresponding zoom of Figure 9 at around 376 seconds shows the maximum absolute estimation error within the entire dataset. Points like this are often correlated with fluctuations in the wheel speeds caused by wheel locking (e.g., due to strong braking as in the example) or wheel slip. Other edge cases where the current model may fail include roads with a high bank or slope angle or irregularities in the road surface, for example, kerbs for race track applications. However, these conditions might also be learned by the model, by providing many such examples in the training dataset. Additionally, in order to reduce the error occurring in these situations, a more accurate speed estimator both for wheel speeds and vehicle speed or other CAN bus signals can be integrated into the side-slip estimator as a feature signal, thereby increasing model robustness.

Furthermore, sensitivity analyses were carried out comparing the prediction results in different grip or wear conditions and maneuvers. For this purpose, Table 4 summarizes the prediction metrics regrouped into the different grip and wear level combinations as in Table 1, while Table 5 shows the prediction metrics according to the maneuver classes in Table 2.

As a result, considering the RMSE value, the same model can achieve good performance on all the combinations of grip and wear conditions considered with no need to change model parameters or perform a new model calibration.

Considering the coefficient of determination R^2, the model performs best in the wet/worn dataset while it has worse performance in the dry/new (a.) dataset. It is interesting to observe that while the model has a high goodness-of-fit in terms of R^2 for the dataset dry/worn (b.), the highest RMSE and the max abs error values are also achieved in this dataset (i.e., 0.18 and 1.52 deg, respectively). This can be justified by considering the dataset distribution in Figure 4, showing a relatively higher share of large β values in dataset b. compared to the other three groups. It is therefore reasonable to expect slightly higher absolute errors and RMSEs in this dataset, despite a lower relative error as expressed by $1 - R^2$. By reverting this logic, referring to Figure 5 and Table 5, it can be clarified why the model has the lowest R^2 in the dataset DLC, while simultaneously exhibiting the lowest RMSE in the same group. From Tables 4 and 1, it can be also observed that, the combinations b., c., and d. show a low RMSE despite being underrepresented in the overall dataset compared to combination a. Summarizing, the RMSE on the overall dataset is about 0.16 deg. The RMSE of this model is similar to the claimed 1σ-accuracy of the ground-truth side-slip angle determined by the OxTS platform, ranging between 0.15 and 0.2 deg [33]. Hence, it can be stated that the model is robust, and it has good performance.

In addition, the dynamic model behavior was analyzed. This was evaluated by estimating the transfer function between the SSE and the target signal. A corresponding Bode diagram in semi-logarithmic scale is presented in Figure 12.

Defining the transfer function as:

$$\left|G(j\omega)\right| = \frac{\text{SSE prediction}}{\text{Target value}} \qquad \text{Eq. (10)}$$

the system displacement gain magnitude expressed in decibel (dB) as well as the phase displacement in degrees can be determined according to

$$\text{Magnitude}\,(\text{dB}) = 20 \cdot \log_{10}\left(\left|G(j\omega)\right|\right)$$

$$\text{Phase}\,(\text{deg}) = \arg\left|G(j\omega)\right| \qquad \text{Eq. (11)}$$

Considering Figure 3, the main frequency content of the model input and target signal is between 0 Hz and 3 Hz. For a proper dynamic behavior of the virtual sensor, the transfer function between model output and target value estimated above should have a magnitude and a phase displacement close to zero within this frequency range, as shown in Figure 12.

Finally, the SSE has been deployed to a dSpace Microautobox II available in the target vehicle under study. On

Downloaded from SAE International by Tiziano Giuliacci, Monday, October 02, 2023

FIGURE 11 Zoom corresponding to Figure 9, showing the maximum absolute estimation error in the dataset.

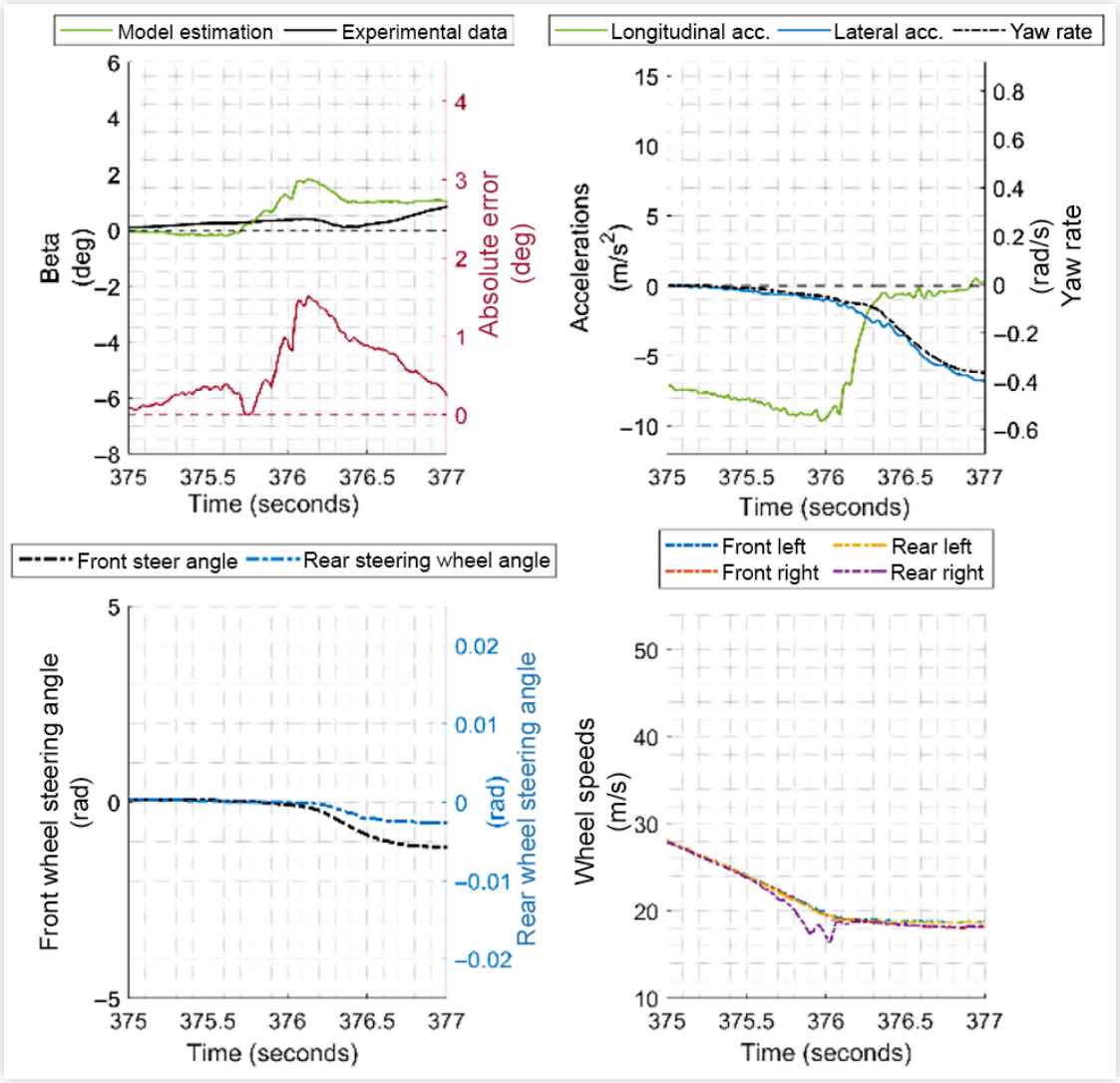

© Addfor S.p.A.

TABLE 4 Prediction metrics for different tire grip and wear conditions.

Overall dataset				
	Condition Grip/wear level	RMSE (deg)	R^2 (-)	Max abs error (deg)
a.	Dry/new	0.17	0.90	1.28
b.	Dry/worn	0.18	0.97	1.52
c.	Wet/new	0.15	0.93	1.06
d.	Wet/worn	0.12	0.98	0.97

© Addfor S.p.A.

TABLE 5 Prediction metrics for different maneuver types.

Overall dataset				
	Maneuver	RMSE (deg)	R^2 (-)	Max abs error (deg)
A.	Steer sinus sweep	0.04	0.96	0.18
B.	Circle	0.21	0.98	0.96
C.	Steer ramp	0.22	0.97	1.28
D.	DLC	0.07	0.81	0.36
E.	Handling	0.17	0.95	1.52

© Addfor S.p.A.

Downloaded from SAE International by Tiziano Giuliacci, Monday, October 02, 2023

FIGURE 12 Model frequency response.

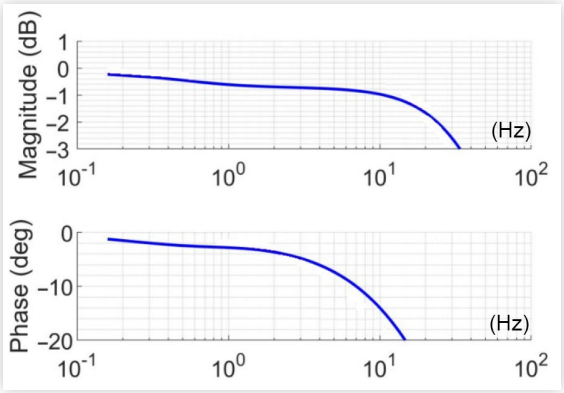

this platform, setting a cycle time of 10 ms, a real-time factor of greater than 5 could be achieved, thereby confirming the real-time capability of the presented virtual side-slip estimator.

Conclusion

This study deals with a stand-alone RNN model for real-time on-board vehicle side-slip angle estimation. The system uses only signals available on most production vehicles and returns a time-discrete side-slip angle estimate at a predefined frequency (e.g., 100 Hz for the reported application). The model has been trained and tested through on-road data acquisition with a front and rear wheel steering vehicle in different working conditions regarding tire wear and grip. Final tests showed that the proposed method is consistent, with high performance and small errors in the overall considered conditions.

The model described is a black box, and after the training it can be applied only to vehicles with similar kinematic and dynamic properties, otherwise a new training process is required.

Future research could investigate the possibility of enhancing the model's operational domain including vehicles with different characteristics without requiring a new training, resulting in a parametrizable model. Furthermore, this model may be integrated with stability control systems or may be exploited for different applications such as the friction estimation between road and tires. The model could also be validated on several additional working conditions, for example, snow and ice road surfaces or different tire sizes or material. Further applications of the SSE (which cannot be shown here because of confidential data) have already shown a good model performance in these cases.

Once the NN has been trained and tested, the software is light enough to be embedded in an on-board vehicle ECU and to share the virtual sensor predictions with vehicle stability management functions.

Contact Information

Tiziano Alberto Giuliacci
corresponding author
tiziano.giuliacci@add-for.com
https://orcid.org/0000-0002-9502-1079

Stefano Ballesio
stefano.ballesio@add-for.com

Marco Fainello
marco.fainello@add-for.com

Ulrich Mair
Ulrich.Mair@zf.com

Julian King
Julian.King@zf.com
https://orcid.org/0000-0003-3648-9787

References

1. Nishio, A., Tozu, K., Yamaguchi, H., Asano, K. et al., "Development of Vehicle Stability Control System Based on Vehicle Sideslip Angle Estimation," SAE Technical Paper 2001-01-0137 (2001), doi:https://doi.org/10.4271/2001-01-0137.
2. Fukada, Y., "Slip-Angle Estimation for Vehicle Stability Control, Vehicle System Dynamics," *International Journal of Vehicle Mechanics and Mobility* 32, no. 4-5 (1999): 375-388, doi:10.1076/vesd.32.4.375.2079.
3. Piyabongkarn, D., Rajamani, R., Grogg, J.A., and Lew, J.Y., "Development and Experimental Evaluation of a Slip Angle Estimator for Vehicle Stability Control," *IEEE Transactions on Control Systems Technology* 17, no. 1 (2009): 78-88, doi:10.1109/TCST.2008.922503.
4. Ishak, M.I., Ogino, H., and Yamamoto, Y., "Numerical Simulation Analysis of an Oversteer In-Wheel Small Electric Vehicle Integrated with Four-Wheel Drive and Independent Steering," *International Journal of Vehicular Technology* 2016 (2016): 12, doi:10.1155/2016/7235471.
5. Chunyun, F., Hoseinnezhad, R., Bab-Hadiashar, A., and Jazar, R.N., "Electric Vehicle Side-Slip Control via Electronic Differential," *International Journal of Vehicle Autonomous Systems* 13, no. 1 (2015): 1-26, doi:10.1504/IJVAS.2015.070724.
6. Hać, A.B. and Bedner, E.J., "Robustness of Side Slip Estimation and Control Algorithms for Vehicle Chassis Control," in *Proceedings of the 20th International Technical Conference on the Enhanced Safety of Vehicles*, Lyon, France, 2007.

Downloaded from SAE International by Tiziano Giuliacci, Monday, October 02, 2023

7. Bian, M., Chen, L., Luo, Y., and Li, K., "A Dynamic Model for Tire/Road Friction Estimation under Combined Longitudinal/Lateral Slip Situation," SAE Technical Paper 2014-01-0123 (2014), doi:https://doi.org/10.4271/2014-01-0123.
8. Shao, L., Jin, C., Lex, C., and Eichberger, A., "Nonlinear Adaptive Observer for Side Slip Angle and Road Friction Estimation," in *Proceedings of the 2016 IEEE 55th Conference on Decision and Control*, Las Vegas, NV, 2016, 6258-6265, doi:10.1109/CDC.2016.7799232.
9. Ping, X., Cheng, S., Yue, W., Du, Y. et al., "Adaptive Estimations of Tyre-Road Friction Coefficient and Body's Sideslip Angle Based on Strong Tracking and Interactive Multiple Model Theories," *Proceedings of the Institution of Mechanical Engineers* 234, no. 14 (2020): 3224-3238, doi:10.1177/0954407020941410.
10. Rosen, I., "Tire Wear Modeling," *Transport Problems* 11, no. 3 (2016): 111-120, doi:10.20858/tp.2016.11.3.11.
11. Ziaukas, Z., Busch, A., and Wielitzka, M., "Estimation of Vehicle Side-Slip Angle at Varying Road Friction Coefficients Using a Recurrent Artificial Neural Network," in *Proceedings of the IEEE Conference on Control Technology and Applications*, San Diego, CA, 2021, 986-991, doi:10.1109/CCTA48906.2021.9658710.
12. Kabadayi, S., Pridgen, A., and Julien, C., "Virtual Sensors: Abstracting Data from Physical Sensors," in *Proceedings of the 2006 International Symposium on a World of Wireless, Mobile and Multimedia Networks*, vol. 592, Buffalo-Niagara Falls, NY, 2006, doi:10.1109/WOWMOM.2006.115.
13. Singh, K.B., Arat, M.A., and Taheri, S., "Literature Review and Fundamental Approaches for Vehicle and Tire State Estimation," *Vehicle System Dynamics* 57, no. 11 (2019): 1643-1665, doi:10.1080/00423114.2018.1544373.
14. Chen, B.-C. and Hsieh, F.-C., "Sideslip Angle Estimation Using Extended Kalman Filter," *Vehicle System Dynamics* 46 (2008): 353-364, doi:10.1080/00423110801958550.
15. Li, L., Jia, G., Ran, X. et al., "A Variable Structure Extended Kalman Filter for Vehicle Sideslip Angle Estimation on a Low Friction Road," *Vehicle System Dynamics* 52 (2014): 280-308, doi:10.1080/00423114.2013.877148.
16. Syed, U. and Vigliani, A., "Vehicle Side Slip and Roll Angle Estimation," SAE Technical Paper 2016-01-1654 (2016), doi:https://doi.org/10.4271/2016-01-1654.
17. Singh, K.B., "Vehicle Sideslip Angle Estimation Based on Tire Model Adaptation," *Electronics* 8 (2019): 199, doi:10.3390/electronics8020199.
18. Li, J. and Zhang, J.-X., "Vehicle Sideslip Angle Estimation Based on Hybrid Kalman Filter," *Mathematical Problems in Engineering* 2016 (2016): 10, doi:10.1155/2016/3269142.
19. Selmanaj, D., Corno, M., Panzani, G., and Savaresi, S.M., "Vehicle Sideslip Estimation: A Kinematic Based Approach," *Control Engineering Practice* 67 (2017): 1-12, doi:10.1016/j.conengprac.2017.06.013.
20. How, J., Pohlman, N., and Park, C., "GPS Estimation Algorithms for Precise Velocity, Slip and Race-Track Position Measurements," SAE Technical Paper 2002-01-3336 (2002), doi:https://doi.org/10.4271/2002-01-3336.
21. Li, X., Xu, N., Li, Q., Guo, K. et al., "A Fusion Methodology for Sideslip Angle Estimation on the Basis of Kinematics-Based and Model-Based Approaches," *Proceedings of the Institution of Mechanical Engineers* 234, no. 7 (2020): 1930-1943, doi:10.1177/0954407019892156.
22. Li, X., Chan, C., and Wang, Y., "A Reliable Fusion Methodology for Simultaneous Estimation of Vehicle Sideslip and Yaw Angles," *IEEE Transactions on Vehicular Technology* 65, no. 6 (2016): 4440-4458, doi:10.1109/TVT.2015.2496969.
23. Liu, W., Xiong, L., Xia, X., and Yu, Z., "Vehicle Sideslip Angle Estimation: A Review," SAE Technical Paper 2018-01-0569 (2018), doi:https://doi.org/10.4271/2018-01-0569.
24. Joanny, S., Ali, C., and Dominique, M., "Experimental Evaluation of Vehicle Sideslip Angle Observers," *IFAC Proceedings Volumes* 37, no. 8 (2004): 275-280, doi:10.1016/S1474-6670(17)31988-2.
25. Lenain, R., Thuilot, B., Cariou, C., and Martinet, P., "Mixed Kinematic and Dynamic Sideslip Angle Observer for Accurate Control of Fast Off-Road Mobile Robots," *Journal of Field Robotics* 27, no. 2 (2010): 181-196, doi:10.1002/rob.20319ff. ffhal-00523387f.
26. Liao, Y.-W. and Borrelli, F., "An Adaptive Approach to Real-Time Estimation of Vehicle Sideslip, Road Bank Angles and Sensor Bias," *IEEE Transactions on Vehicular Technology* 68, no. 8 (2019): 7443-7454, doi:10.1109/TVT.2019.2919129.
27. Chindamo, D. and Gadola, M., "Estimation of Vehicle Side-Slip Angle Using an Artificial Neural Network," *Proceedings of the MATEC Web of Conferences* 166 (2018): 02001, doi:10.1051/matecconf/201816602001.
28. Park, Y., Gajamannage, K., Jayathilake, D.I., and Bollt, E.M., "Recurrent Neural Networks for Dynamical Systems: Applications to Ordinary Differential Equations, Collective Motion, and Hydrological Modeling," *Chaos: An Interdisciplinary Journal of Nonlinear Science* 33 (2023): 013109, doi:10.48550/arXiv.2202.07022.
29. Liang, Y., Müller, S., Rolle, D., Ganesch, D. et al., "Vehicle Side-Slip Angle Estimation with Deep Neural Network and Sensor Data Fusion," in *Proceedings of the 10th International Munich Chassis Symposium*, Munich, Germany, 2019, 159-178, doi:10.1007/978-3-658-26435-2_15.
30. Novi, T., Capitani, R., and Annicchiarico, C., "An Integrated Artificial Neural Network–Unscented Kalman Filter Vehicle Sideslip Angle Estimation Based on Inertial Measurement Unit Measurements," *Proceedings of the Institution of Mechanical Engineers* 233, no. 7 (2019): 1864-1878, doi:10.1177/095440701879064.

Downloaded from SAE International by Tiziano Giuliacci, Monday, October 02, 2023

31. Chindamo, D., Lenzo, B., and Gadola, M., "On the Vehicle Sideslip Angle Estimation: A Literature Review of Methods, Models, and Innovations," *Applied Sciences* 8, no. 3 (2018): 355, doi:10.3390/app8030355.

32. Liu, J., Wang, Z., Zhang, L., and Walker, P., "Sideslip Angle Estimation of Ground Vehicles: A Comparative Study," *IET Control Theory & Applications* 14, no. 20 (2021): 3490-3505, doi:10.1049/iet-cta.2020.0516.

33. RT3000 v3, "RT3000-v3-datasheet-201023_web.pdf," accessed May 2023, http://www.oxts.com/wp-content/uploads/2020/11/RT3000-v3-datasheet-201023_web.pdf.

34. Gers, F.A., Schmidhuber, J., and Cummins, F., "Learning to Forget: Continual Prediction with LSTM," in *Proceedings of the 1999 Ninth International Conference on Artificial Neural Networks 99*, No. 470, Edinburgh, UK, 1999, 850-855, doi:10.1049/cp:19991218.

© 2024 Addfor S.p.A. Published by SAE International. This Open Access article is published under the terms of the Creative Commons Attribution License (http://creativecommons.org/licenses/by/4.0/), which permits distribution, and reproduction in any medium, provided that the original author(s) and the source are credited.

Positions and opinions advanced in this work are those of the author(s) and not necessarily those of SAE International. Responsibility for the content of the work lies solely with the author(s).